

Environmental effects on vibrational proton dynamics in H_5O_2^+ : DFT study on crystalline $\text{H}_5\text{O}_2^+\text{ClO}_4^-$

Mikhail V. Vener and Joachim Sauer*

Institut für Chemie, Humboldt-Universität zu Berlin, Unter den Linden 6, 10099 Berlin, Germany

Received 18th August 2004, Accepted 18th November 2004
First published as an Advance Article on the web 10th December 2004

The structure as well as IR and inelastic neutron scattering (INS) spectra of H_5O_2^+ in crystalline $\text{H}_5\text{O}_2^+\text{ClO}_4^-$ were simulated using Car–Parrinello molecular dynamics with the BLYP functional. The potential of the $\text{O}\cdots\text{H}^+\cdots\text{O}$ fragment is very shallow. The $Pnma$ structure, assumed in the X-ray study to be the most suitable choice, is a saddle point on the potential energy surface, while the $P2_12_12_1$ minimum structure is only 20 cm^{-1} lower in energy. The computed INS and IR spectra enable us to achieve a complete assignment of the observed spectra. The broad band between 1000 and 1400 cm^{-1} is due to the asymmetric stretch and one of the bending vibrations of the $\text{O}\cdots\text{H}^+\cdots\text{O}$ fragment, while the band between 1600 and 1800 cm^{-1} is due to the bending vibration of the water molecules and the second bending of the $\text{O}\cdots\text{H}^+\cdots\text{O}$ fragment. Comparison with the vibrational spectra of isolated H_5O_2^+ , obtained using Born–Oppenheimer molecular dynamics simulation, reveals environmental effects on vibrational proton dynamics in strong H-bonded species. The most pronounced changes are found for the $\text{O}\cdots\text{H}^+\cdots\text{O}$ bending modes because the two bending coordinates become distinctly different for the structure that the H_5O_2^+ ion assumes in the crystal.

1. Introduction

H_5O_2^+ is a prototype of strongly H-bonded systems, which plays an important role in condensed phase^{1–3} and enzymatic reactions.⁴ Experimental^{5–7} and theoretical^{8–12} studies of dynamics of the excess proton in water provide valuable insight in the proton transfer phenomenon in polar solvents. This resulted in a qualitative or semi-quantitative picture that is still incomplete and controversial because of the limited applicability of diffraction methods and the technical limitations of molecular dynamics (MD) simulations. In contrast to solvents, molecular crystals provide a better defined environment for the H_5O_2^+ species. In crystalline $\text{H}_5\text{O}_2^+\text{ClO}_4^-$ the H_5O_2^+ structure was determined by X-ray diffraction.¹³ Infrared (IR), Raman and incoherent inelastic neutron scattering (INS) spectra are also available for this system.^{14,15} The IR spectrum of gas phase H_5O_2^+ has only recently been measured.¹⁶ Car–Parrinello molecular dynamics (CPMD)^{17,18} provides a unique possibility to study the effect of the crystalline environment on the structure and dynamics of H_5O_2^+ when one accepts the limited accuracy of density functional theory (DFT), see ref. 19 for a recent example. We use CPMD to simulate the structure as well INS and IR spectra of H_5O_2^+ in the $\text{H}_5\text{O}_2^+\text{ClO}_4^-$ crystal and compare it with the H_5O_2^+ gas-phase species. The discussion addresses the following issues: (i) the environmental effects on the structure and vibrational spectra of H_5O_2^+ ; (ii) the relationship between the IR and INS spectra, specifically the broad IR bands compared to relatively narrow INS bands for the $\text{O}\cdots\text{H}^+\cdots\text{O}$ vibrations.²⁰

2. Computations

For the isolated H_5O_2^+ ion in the gas phase Born–Oppenheimer molecular dynamics simulations were made with DFT forces (AIMD)^{21,22} using the TURBOMOLE package (V5-6)^{23–25} The forces were calculated analytically using the BLYP functional²⁶ and the aug-cc-pVTZ basis set.²⁷ NVE simulations were performed such that the average of the kinetic energy corresponds to a temperature of about 100 K . The

equilibrium structure was used as a starting point. Inertial momenta were distributed randomly according to the desired kinetic temperature. The time step was 0.5 fs and the trajectory length was 3 ps . Vibrational spectra were calculated by averaging over two trajectories, obtained with opposite signs of the starting velocities.

The CPMD calculations use the BLYP functional²⁶ with Trouillier–Martins²⁸ pseudo-potentials for core electrons. The kinetic energy cutoff for the plane wave basis set is 80 Ry and k -space sampling is limited to the Γ point. These values yield structures and harmonic frequencies of the isolated H_5O_2^+ and ClO_4^- ions that are comparable to BLYP results obtained with the aug-cc-pVTZ Gaussian basis sets.²⁷ For example, for the $\text{O}\cdots\text{O}$ and O–H distances and the $\text{O}\cdots\text{H}\cdots\text{O}$ angle the Gaussian/plane wave results (Å , degree) are $2.43/2.43$, $0.979/0.980$ and $172.8/174.1$, respectively. Also both approaches yield within 1 kJ mol^{-1} the same energy²⁹ for dissociating H_5O_2^+ into H_3O^+ and H_2O , 147 kJ mol^{-1} .

In dynamic runs a fictitious electron mass of 600 au and a time step of 5 au ($\approx 0.12\text{ fs}$) were employed.³⁰ NVT simulations were performed at constant volume and for $T = 84\text{ K}$, the average temperature in different experimental studies of crystalline $\text{H}_5\text{O}_2^+\text{ClO}_4^-$.^{13–15} The BLYP equilibrium geometry was used as a starting point. The trajectory length was 4.5 ps . To obtain the IR and INS spectra the average was taken over two trajectories computed with different values of the thermostat frequency,¹⁸ 2000 and 3500 cm^{-1} . The dipole moment function was obtained by the Berry phase approach of Resta³¹ as implemented in CPMD.¹⁸

The IR spectrum was obtained as the Fourier transform of the autocorrelation function of the classical dipole moment, M ,³²

$$I(\omega) = \left(\frac{2\pi\omega}{\epsilon_0 c h n} \right) F(\omega) \text{Re} \int_0^\infty e^{i\omega t} \langle M(t)M(0) \rangle dt \quad (1)$$

where $I(\omega)$ is the relative IR absorption at frequency ω , T is the

temperature, k_B is the Boltzmann constant, c is the speed of light in vacuum, ϵ_0 is the dielectric constant of the vacuum, and n is the refractive index which was treated as constant.

The function $F(\omega)$ results from the prefactor of the classical line shape and from a quantum correction factor which corrects for the violation of the detailed balance conditions in the classical treatment and for zero point motion effects. Unfortunately, there exist a large variety of different suggestions which are discussed in detail, for example, by Gaigeot and Sprik³³ who also compare IR spectra obtained with different choices. We consider here the 'standard' quantum correction factor $2/(1 + \exp(-h\omega/2\pi k_B T))$,^{33,34} which results in

$$F(\omega) = 2 \tanh\left(\frac{h\omega}{4\pi k_B T}\right) \quad (2a)$$

It has previously been applied in calculations of the far and mid-IR spectra of liquid water^{32,34} and crystals.³⁵ In addition, comparison will be made with the so-called 'harmonic' quantum correction factor $h\omega/2\pi k_B T/(1 - \exp(-h\omega/2\pi k_B T))$ which yields

$$F(\omega) = \frac{h\omega}{2\pi k_B T} \quad (2b)$$

The INS spectrum was calculated from the Fourier transform of the velocity autocorrelation functions of the atoms, weighted by their inelastic neutron scattering cross-sections.³⁶ Since the value of the INS cross-section of the H atom is, at least, one order of magnitude larger than that of the C, O and Cl atoms, only the H atom velocities, v_H were taken into account,

$$I(\omega) = \left(\frac{4\pi\omega}{\epsilon_0 c h n}\right) \tanh\left(\frac{h\omega}{4\pi k_B T}\right) \text{Re} \int_0^\infty e^{i\omega t} \langle v_H(t) v_H(0) \rangle dt \quad (3)$$

3. Crystal structure and harmonic frequencies

Dimensions of the unit cell, which contains four formula units of $\text{HClO}_4 \cdot 2\text{H}_2\text{O}$, as well as the positions of the heavy atoms, were taken from ref. 13. Positions of H atoms which are not available from experiment were obtained following the Olovsson prescriptions.¹³ Optimisation of all atomic positions yields a structure with four equivalent $\text{H}_5\text{O}_2^+ \text{ClO}_4^-$ units. In accord with the experimental data, the CPMD results suggest a structure in which the proton of the perchloric acid has been transferred to water and is shared by two water molecules, forming the H_5O_2^+ ions. These H_5O_2^+ ions are hydrogen bonded to the ClO_4^- ions. There are no hydrogen bonds between different H_5O_2^+ ions. The theoretical crystal structure (under the assumption of fixed cell parameters) is orthorhombic, space group $P2_12_12_1$ (no. 19). This was verified by a vibrational analysis which does not show imaginary frequencies. It should be noted that the X-ray study¹³ considered the non-centrosymmetric $Pn2_1a$ structure as a possible choice, but the centrosymmetric space group $Pnma$ (no. 62) was accepted as most suitable. We find that the latter corresponds to a transition structure with one imaginary frequency (78 cm^{-1}). The transition



corresponds to a simultaneous shift of the four bridging protons along the $\text{O} \cdots \text{O}$ line. The $\text{O} \cdots \text{H}$ distances in the $\text{O} \cdots \text{H}^+ \cdots \text{O}$ fragment of H_5O_2^+ are equal in the transition structure, but differ in the energy minimum structure. The corresponding Cl–O distances in the two structures differ by less than 0.001 \AA , while the $\text{O} \cdots \text{O}$ distances differ by up to

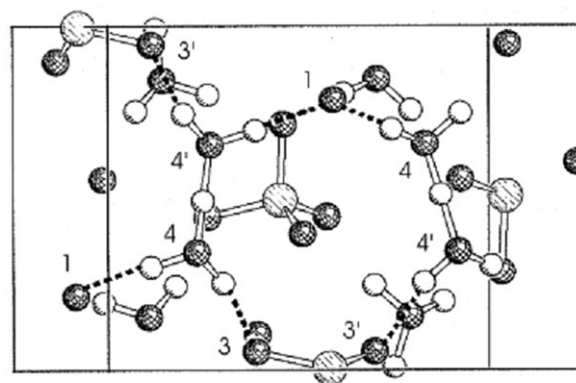


Fig. 1 Crystal structure of $\text{H}_5\text{O}_2^+ \text{ClO}_4^-$ calculated by DFT (Schäkal³⁴ drawing). Open circles represent hydrogen atoms, large light grey circles chlorine atoms and small dark grey circles oxygen atoms. Numbering of O atoms according to ref. 12. Oxygen atoms O(2), that are not involved in H-bonding, are not numbered. Hydrogen bonds are indicated by dashed lines.

0.03 \AA . The energy difference between the two structures is $\approx 20 \text{ cm}^{-1}$, i.e. less than $k_B T$ at experimental temperature.³⁷

Fig. 1 shows the calculated crystal structure. The oxygen atoms of the ClO_4^- ion, labeled O(1), O(2), O(3) and O(3'), are connected *via* H-bonds to oxygen atoms of H_5O_2^+ , labeled as O(4) and O(4'). Oxygen O(1) is acceptor of two H-bonds, O(3) and O(3') accept one, whereas O(2) is not involved in any H-bond ($\text{O}(2) \cdots \text{O}(4)$ distance $> 3.2 \text{ \AA}$). Calculated bond distances are compared with X-ray results in Table 1. The Cl–O distances are systematically longer than the X-ray values. The Cl–O(1) distance to the oxygen with the highest coordination is somewhat longer than the others. In accord with the X-ray data, water oxygen atoms O(4) and O(4') are pyramidally surrounded by three oxygen neighbours. The $\text{O}(4) \cdots \text{H} \cdots \text{O}(4')$ fragment is virtually linear and the bridging H is not in the middle, but shifted towards O(4). The $\text{O}(4) \cdots \text{H} \cdots \text{O}(4')$ hydrogen bond is very strong as indicated by a very short $\text{O}(4) \cdots \text{O}(4')$ distance (2.426 \AA). H-bonds between the H_5O_2^+ and ClO_4^- ions are relatively weak, their distance varies from 2.72 to 2.78 \AA .

The harmonic frequencies of the isolated H_5O_2^+ ion and the H_5O_2^+ ion in the $\text{H}_5\text{O}_2^+ \text{ClO}_4^-$ crystal are given in Table 2. For the H_5O_2^+ ion in the $\text{H}_5\text{O}_2^+ \text{ClO}_4^-$ crystal stretching and bending vibrations of lateral water molecules are in the ranges 3214 – 3428 and 1671 – 1703 cm^{-1} , respectively. The corresponding bands in the experimental IR spectrum (Fig. 2a)¹⁴ have maxima at $3200/3300$ and at 1700 cm^{-1} , respectively. Harmonic frequencies of the asymmetric stretch of the $\text{O} \cdots \text{H}^+ \cdots \text{O}$ fragment vary from 1023 to 1237 cm^{-1} in the crystal. This may be explained by strong electrostatic interactions between neighbouring $\text{O} \cdots \text{H}^+ \cdots \text{O}$ fragments. The distance between the nearest bridging protons is around 5.3 \AA . The frequencies of one of the two bending vibrations are between 1037 and 1198 cm^{-1} and this range overlaps with the range of the asymmetric stretches of the $\text{O} \cdots \text{H}^+ \cdots \text{O}$ fragment. The frequencies of the

Table 1 Comparison of the calculated bond distances (\AA) in the $P2_12_12_1$ structure with available X-ray diffraction data¹³

Covalent bonds	Calculated, CPMD	X-ray ¹³
Cl–O(1)	1.505	1.458
Cl–O(2)	1.459	1.433
Cl–O(3), Cl–O(3')	1.475, 1.477	1.430
Hydrogen bonds		
$\text{O}(4) \cdots \text{H} \cdots \text{O}(4')$	2.426	2.424
$\text{O}(4) \cdots \text{H} \cdots \text{O}(1)$, $\text{O}(4') \cdots \text{H} \cdots \text{O}(1)$	2.724; 2.781	2.784
$\text{O}(4) \cdots \text{H} \cdots \text{O}(3)$, $\text{O}(4') \cdots \text{H} \cdots \text{O}(3')$	2.755; 2.776	2.788
$\text{O}(4) \cdots \text{H}$, $\text{O}(4') \cdots \text{H}$	1.161, 1.265	—

Table 2 Comparison of the harmonic frequencies (cm^{-1}) of the isolated H_5O_2^+ ion with those obtained for the crystal^a

Assignment	Isolated H_5O_2^+		H_5O_2^+ in $\text{H}_5\text{O}_2^+\text{ClO}_4^-$ crystal CPMD ^c
	C_2	TURBOMOLE ^b	
H_2O torsion	A	335 (0.01)	} 576 – 610
H_2O wagging	B	480 (0.08)	
H_2O wagging	A	521 (0.04)	
H_2O rocking	A	575 (0.03)	} 768 – 863
H_2O rocking	B	600 (0.01)	
$\text{O}\cdots\text{H}^+\cdots\text{O}$ symm. stretch	A	598 (0.00)	520, 538, 564, 576
$\text{O}\cdots\text{H}^+\cdots\text{O}$ asymm. stretch	B	1059 (1.00)	1023, 1130, 1180, 1237
$\text{O}\cdots\text{H}^+\cdots\text{O}$ bending	B	1422 (0.09)	1037, 1183, 1190, 1198
$\text{O}\cdots\text{H}^+\cdots\text{O}$ bending	A	1499 (0.04)	1710, 1713, 1716, 1727
H_2O symm. bending	A	1665 (0.0)	1622, 1625, 1633, 1643
H_2O asymm. bending	B	1708 (0.32)	1671, 1683, 1634, 1703
O-H stretch	B	3595 (0.07)	3214, 3221, 3229, 3234
O-H stretch	A	3610 (0.00)	3301, 3305, 3311, 3313
O-H stretch	B	3682 (0.08)	3357, 3358, 3358, 3366
O-H stretch	A	3682 (0.11)	3377, 3385, 3389, 3428

^a BLYP functional, force constants calculated numerically (step size 0.01 au in both directions) from analytic gradients. ^b Aug-cc-pVTZ basis sets, TURBOMOLE code, intensities in parentheses. ^c Plane-wave (80 Ry) basis set, CPMD code.

second bending vibrations are in the narrow range of 1727–1740 cm^{-1} – very close to the bending vibrations of the terminal water molecules. Our calculations do not support a previous tentative assignment of the bands¹⁴ observed around 1080 cm^{-1} and in the 1700–1900 cm^{-1} range to bending and to asymmetric stretching vibrations of the $\text{O}\cdots\text{H}^+\cdots\text{O}$ fragment, respectively. According to the present calculations the bands between 1000 and 1400 cm^{-1} are due to the asymmetric stretch and bending vibrations of the $\text{O}\cdots\text{H}^+\cdots\text{O}$ fragment, while the bands between 1600 and 1700 cm^{-1} are due to asymmetric bending vibrations of the terminal water molecules and bend-

ing vibrations of the $\text{O}\cdots\text{H}^+\cdots\text{O}$ fragment. This assignment does not change when anharmonicities are included by MD simulations as shown below.

4. INS and IR spectra

The computed INS spectrum of the $\text{H}_5\text{O}_2^+\text{ClO}_4^-$ crystal agrees well with the experimental one, see panels B and A in Fig. 3. In accord with experiment,¹⁵ there are two groups of bands below 850 cm^{-1} and two bands in the region between 1000 and 2000 cm^{-1} . Because the scattering cross section of the proton exceeds that of other atoms by one order of magnitude, INS selectively probes modes in which H atoms are involved. Separate calculation of the velocity autocorrelation function of

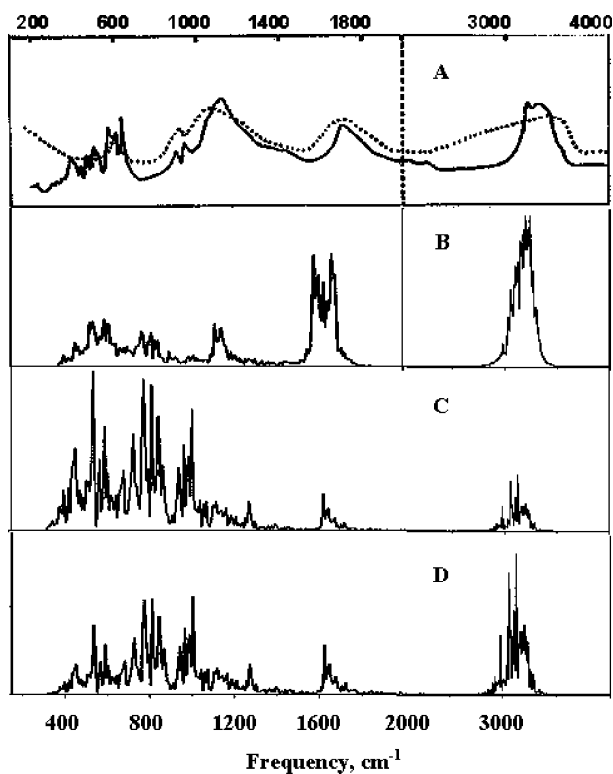


Fig. 2 Computed power (B) and IR (C, D) spectra of crystalline $\text{H}_5\text{O}_2^+\text{ClO}_4^-$ compared to the experimental IR spectrum (A, ref. 14), the dotted line corresponds to the IR spectrum in liquid phase at room temperature.¹⁴ Spectrum C is obtained with the 'standard' quantum correction (eqn. (2a)), spectrum D with the 'harmonic' quantum correction (eqn. (2b)). Intensities are in arbitrary units.

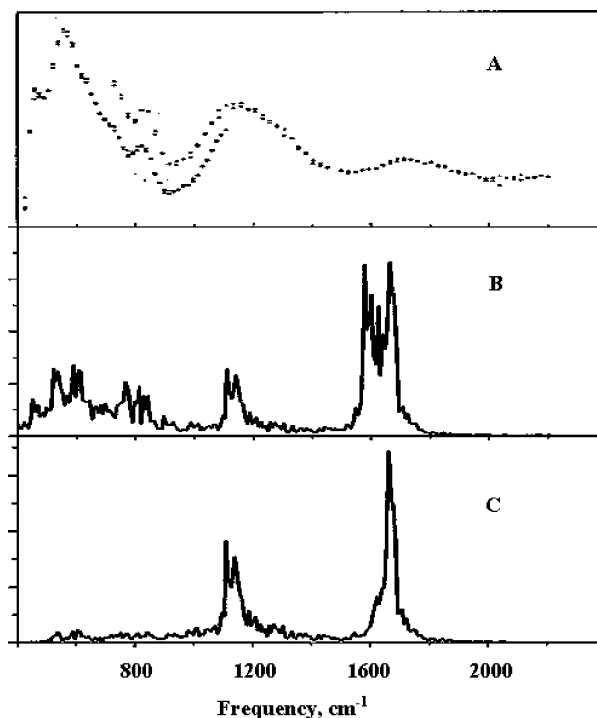


Fig. 3 Experimental (A, ref. 15) and computed (B) INS spectrum of crystalline $\text{H}_5\text{O}_2^+\text{ClO}_4^-$. Panel C shows the INS spectrum computed from the velocity autocorrelation function of the bridging H only. Intensities are in arbitrary units.

the bridging H only (Fig. 3C) allows identification of bands that are due to the O···H⁺···O fragment. Comparison of spectra B and C shows that these are the two bands around 1150 and 1600 cm⁻¹. Further information for the assignment comes from the harmonic frequency normal modes of H₅O₂⁺ in the H₅O₂⁺ClO₄⁻ crystals (Table 2). The bands around 800 cm⁻¹ and around 500 cm⁻¹ correspond to the rocking and wagging vibrations of the terminal water molecules. The intense band around 1150 cm⁻¹ is caused by vibrations of the bridging proton (O···H⁺···O asymm. stretch and O···H⁺···O bend), while the group of the intense bands around 1600 cm⁻¹ is caused by both bending vibrations of the O···H⁺···O fragment and bending vibrations of the terminal water molecules. Comparison of spectra B and C (Fig. 3) shows that the bending vibrations of terminal water molecules are at the low wavenumber side of the band around 1600 cm⁻¹.

Fig. 2 (panels C and D) shows the IR spectrum of the H₅O₂⁺ClO₄⁻ crystal obtained as a Fourier-transform of the dipole autocorrelation function. The power spectrum of the crystal, calculated as the Fourier-transform of the velocity autocorrelation function, is given in the middle panel B of Fig. 2. The latter is usually computed in CPMD studies of vibrational properties of crystals³⁰ and isolated molecules.³⁸ Assignment of the bands in the power spectrum can be made by separate consideration of velocity autocorrelation functions of subsets of atoms. When doing so, we find that all vibrations of the ClO₄⁻ anion locate below 1050 cm⁻¹. The group of bands around 3100 cm⁻¹ corresponds to the OH stretches of the terminal water molecules.

The frequencies obtained from the dipole and velocity autocorrelation functions are close to each other, while intensities of bands differ strongly. According to experiment¹⁴ shown at the top of Fig. 2 the IR intensities of the ClO₄⁻ fundamentals are lower than those of OH stretches of the terminal water molecules and also lower than the other bands, while the present calculations (eqn. (1)) predict the largest IR intensities for the low frequency ClO₄⁻ vibrations when the 'standard' quantum corrections are used (eqn. (2a), panel C). The 'harmoni' quantum correction (eqn. (2b), panel D) increases the intensity of the terminal OH stretches, which are more intense than the ClO₄⁻ vibrations, but the relative intensities of the bands around 1080 cm⁻¹ and between 1700 and 1900 cm⁻¹ is still too low. More sophisticated schemes^{39,40} may lead to a more severe damping for low frequencies as found for liquid water.⁴¹ The observed intensities also depend on the refractive index which in general is frequency dependent.⁴² This dependence is unknown in most cases and has not been considered. We note, however, that for liquid water the refractive index is virtually constant between 300 and 3500 cm⁻¹.⁴³

Following the assignment of the INS spectra (Fig. 3) and the harmonic normal mode calculations (Table 2), the bands in the region between 1600 and 1700 cm⁻¹ are due to asymmetric bending vibrations of the water molecules and the bending vibrations of the O···H⁺···O fragment. The bands in the region between 1000 and 1300 cm⁻¹ are assigned to the asymmetric stretch and bending vibrations of the O···H⁺···O fragment (Table 2). A very broad and flat absorption is observed for the H₅O₂⁺ClO₄⁻ crystal¹⁴ in this region (upper panel in Fig. 2). This is also true for the dehydrates of hydrogen chlorine and hydrogen bromine⁴⁴ as well as for dehydrates of halogenometallates of dioxonium.⁴⁵ Comparison of the theoretical INS and IR spectra of the H₅O₂⁺ClO₄⁻ crystal shows that the O···H⁺···O band around 1150 cm⁻¹ is much broader in the IR spectrum than in the INS one. The band broadening in the IR spectrum is caused by electric anharmonicities^{46,47} in addition to mechanical ones. The electric anharmonicities are absent in the INS spectrum and this explains the narrower bands.

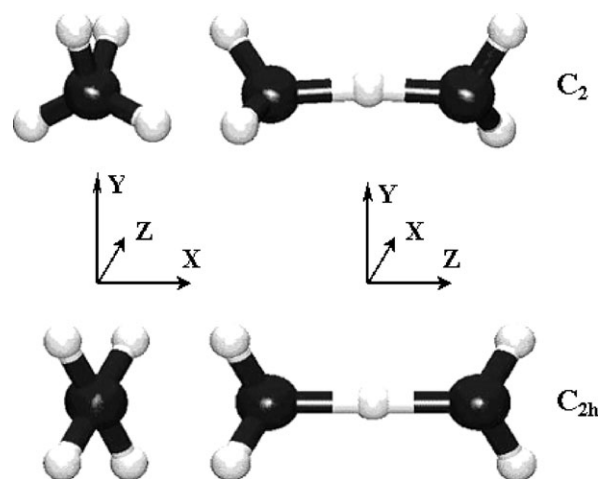


Fig. 4 Structure of H₅O₂⁺ in gas phase (top) and the crystal (bottom). The coordinate origin is at the midpoint between the oxygen atoms on the O···O line, y is the C₂ axis and z is the O···O line.

5. Discussion

The equilibrium O···O distances are 2.431 Å in the isolated ion and 2.426 Å in the crystal, *i.e.* they are virtually the same. The O···H⁺···O fragment is slightly nonlinear in the gas phase (172°) and becomes linear in the crystal. Due to the strength of the O···H⁺···O bond, the crystalline environment changes the O···O distance only slightly.

In the crystal and gas phase the H₅O₂⁺ ion can be considered as a non-rigid molecule because the bridging H undergoes large-amplitude vibrations. The molecular symmetry group of H₅O₂⁺ in the crystal is C_{2h}.⁴⁸ Approximately C_{2h} symmetry of the H₅O₂⁺ ion has also been found in X-ray studies of crystalline hydrates of different acids, *e.g.* ref. 49 and the references therein. The crystalline environment changes the mutual orientation of the water molecules in H₅O₂⁺ compared to the isolated species, see Fig. 4. As a result, in the crystal the bending potential along y increases much faster than along x and the frequencies of the two bending vibrations of the O···H⁺···O fragment differ strongly in the crystal. In contrast, in the gas phase the bending potentials in x- and y-directions are more similar and the two bending modes are virtually degenerate, see Table 2.

We start the discussion of environment effects on the vibrational spectra of the H₅O₂⁺ species with the OH stretch modes of the external water molecule. The simulated IR spectrum of H₅O₂⁺ClO₄⁻ (Fig. 2C) shows these bands between 3000 and 3300 cm⁻¹ while the isolated H₅O₂⁺ ion (simulated spectrum not shown in this region) has bands between 3500 and 3700 cm⁻¹ (with peaks at 3575 and 3685 cm⁻¹). This is in agreement with the observed spectrum of H₅O₂⁺ClO₄⁻ (Fig. 2A) which has maxima at about 3200 and 3300 cm⁻¹ and the spectrum of isolated H₅O₂⁺ which has lines at 3609 and 3684 cm⁻¹.⁵⁰ This shift of about 400 cm⁻¹ (observed) is typical of H-bonds as formed by the terminal OH groups of H₅O₂⁺ with oxygen atoms O(1) and O(3)/O(3') of the ClO₄⁻ ions (Fig. 1). The HOH bendings of the terminal water molecules are part of the broad band around 1700–1800 cm⁻¹ in the simulated spectrum of isolated H₅O₂⁺, which shifts to about 1600–1700 cm⁻¹ in the simulated spectrum of the H₅O₂⁺ClO₄⁻ crystal. The harmonic frequencies also indicate a very small red shift of 4–35 cm⁻¹. The range of 30 cm⁻¹ results from the weak coupling between the four H₅O₂⁺ units in the unit cell.

Comparison of the computed INS spectra of the isolated H₅O₂⁺ ion and the H₅O₂⁺ClO₄⁻ crystal (Fig. 5a, harmonic frequencies shown as sticks) reveals the following environmental effects on the H₅O₂⁺ vibrations: (i) Wagging and rocking vibrations of the terminal water molecules shift to higher

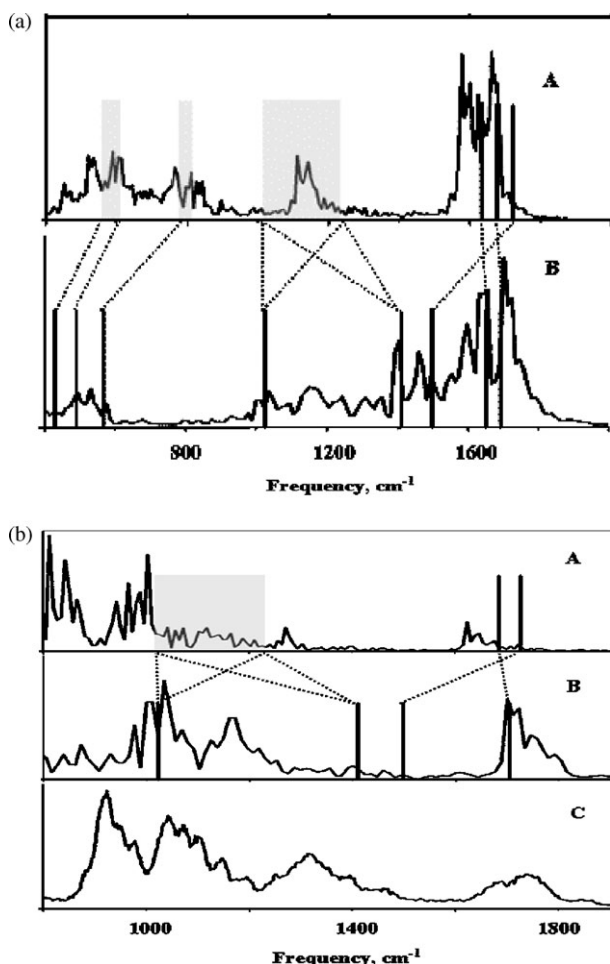


Fig. 5 (a) Computed INS spectra of crystalline $\text{H}_5\text{O}_2^+\text{ClO}_4^-$ (A) and of the isolated H_5O_2^+ ion (B). Intensities are in arbitrary units. Harmonic frequencies are shown as sticks. (b) Computed IR spectrum of the $\text{H}_5\text{O}_2^+\text{ClO}_4^-$ crystals (A) compared with the computed IR spectrum of the H_5O_2^+ ion in the gas phase (B). The 'standard' quantum correction, eqn. (2a), is used. Harmonic frequencies are shown as sticks. The experimental¹⁶ gas phase spectrum in the region between 800 and 2000 cm^{-1} is also shown (C). Intensities are in arbitrary units.

wavenumbers due to the crystalline environment. In the gas phase spectrum the bands around 800 cm^{-1} are absent. (ii) A large number of relatively intense bands in the 1200 to 1600 cm^{-1} region caused by vibrations of the bridging H disappear in the crystal. This is due to a much larger splitting of the two $\text{O}\cdots\text{H}^+\cdots\text{O}$ bending vibrations in the crystal as the harmonic frequencies indicate (1037–1198 and 1727–1740 cm^{-1} compared to 1411 and 1500 cm^{-1} in the gas phase, *cf.* Table 2). In the crystal, the $\text{O}\cdots\text{H}^+\cdots\text{O}$ asymm. stretches of the four H_5O_2^+ fragments are found in the same region (harmonic wavenumbers of 1023–1237 cm^{-1}) as the lower of the $\text{O}\cdots\text{H}^+\cdots\text{O}$ bends (1037–1198 cm^{-1}).

The same frequency shifts determine the environmental effects on the IR spectra (Fig. 5b). However, because of different intensities the spectral changes are different. The $\text{O}\cdots\text{H}^+\cdots\text{O}$ bends which are clearly seen in the computed INS spectrum of the isolated H_5O_2^+ have very low intensity in the computed IR spectrum. In contrast to the asymm. $\text{O}\cdots\text{H}^+\cdots\text{O}$ stretch, these motions yield small changes of the dipole of the $\text{O}\cdots\text{H}^+\cdots\text{O}$ fragment. It is therefore very likely that the $\text{O}\cdots\text{H}^+\cdots\text{O}$ bends also contribute little to the IR spectrum of the $\text{H}_5\text{O}_2^+\text{ClO}_4^-$ crystal.

Comparison of the experimental IR spectrum of the isolated H_5O_2^+ ion¹⁶ (panel C in Fig. 5b) and the ion in crystal (panel A in Fig. 2) shows that the positions of the broad bands around 1000–1200 and 1600–1800 cm^{-1} are slightly affected by the

crystalline environment, while the band around 1300 cm^{-1} in the gas phase spectrum almost disappears in the crystal and only a shoulder remains around 1400 cm^{-1} .

Comparison of the computed INS and IR spectra for the gas phase species (panels B in Figs. 5a and b) shows that the $\text{O}\cdots\text{H}^+\cdots\text{O}$ bends are seen in the simulated INS spectrum (Fig. 5a, left) at slightly lower wavenumbers compared to harmonic ones, but they are not seen in the simulated IR spectrum (Fig. 5b, right). This is due to relatively small changes of the dipole moment associated with $\text{O}\cdots\text{H}^+\cdots\text{O}$ bendings. Therefore, it is likely that they do not show up in the experimental gas phase spectrum of H_5O_2^+ , *cf.* ref. 51. The two middle bands in the experimental IR spectrum may then be due to overtones or combination bands^{46,52} which gain intensity from strong electric and mechanical anharmonicity.⁴⁶

6. Summary and conclusions

In accord with experimental data, the present DFT calculations suggest the presence of H_5O_2^+ ions in $\text{HClO}_4\cdot 2\text{H}_2\text{O}$ crystals. The terminal OH groups form hydrogen bonds with the ClO_4^- anions. The potential for the bridged proton in H_5O_2^+ is very shallow. The *Pnma* structure is a saddle point, but the *P2₁2₁2₁* minimum structure is only 20 cm^{-1} lower in energy. The INS and IR spectra have been obtained from a molecular dynamics simulation and a complete assignment of the observed spectra^{14,15} has been achieved. The assignment has been supported by normal mode analysis which shows that anharmonicities of the potential do not have a qualitative effect on the spectrum. Contrary to a previous assignment,¹⁴ the broad band between 1000 and 1400 cm^{-1} seen in the INS and IR spectra of $\text{H}_5\text{O}_2^+\text{ClO}_4^-$ is due to both the asymmetric stretch and one of the bending vibrations of the $\text{O}\cdots\text{H}^+\cdots\text{O}$ fragment, while the band between 1600 and 1800 cm^{-1} is due to both the asymmetric bending vibration of the water molecules and the second bending vibrations of the $\text{O}\cdots\text{H}^+\cdots\text{O}$ fragment. Similarly, all bands of the vibrational spectrum of crystalline benzoic acid have recently been assigned based on the harmonic approximation and DFT calculations.⁵³

Comparison with MD simulations of the INS and IR spectra of isolated H_5O_2^+ ions reveals the environmental effects on the H_5O_2^+ ion in the crystal. As expected, the terminal OH stretching modes are red-shifted by about 400 cm^{-1} due to H-bonding with O atoms of the ClO_4^- ions. The wagging and rocking modes of the terminal water molecules, which are between 400 and 600 cm^{-1} in the gas phase species, are blue shifted to a different degree and give rise to two separated peaks in the INS spectrum around 600 and 800 cm^{-1} , respectively. The bending modes of the terminal H_2O molecules stay around 1600–1700 cm^{-1} . The most pronounced changes of the spectrum occur for the asymmetric stretching and bending modes of the bridging proton. In the gas phase species, the two $\text{O}\cdots\text{H}^+\cdots\text{O}$ bendings are almost degenerate and locate between the asymm. $\text{O}\cdots\text{H}^+\cdots\text{O}$ stretching (1000–1200 cm^{-1}) and the bendings of the terminal water molecules (1700–1800 cm^{-1}). In the crystal they split, because the two bending coordinates are no longer equivalent for the geometry that H_5O_2^+ has in the crystal environment. The splitting is so large that one of the bendings gets very close to the bendings of the terminal water molecules, while the other overlaps with the asymm. $\text{O}\cdots\text{H}^+\cdots\text{O}$ stretching. The harmonic frequencies of both the asymm. $\text{O}\cdots\text{H}^+\cdots\text{O}$ stretchings and the overlapping $\text{O}\cdots\text{H}^+\cdots\text{O}$ bendings of the four H_5O_2^+ fragments cover a broad range between 1000 and 1200 cm^{-1} .

Acknowledgements

This work has been supported by the 'Fonds der Chemischen Industrie' and 'Deutsche Forschungsgemeinschaft'. Computer time on the Cray T3E at the Zentrum für Informationstechnik

Berlin is gratefully acknowledged. We thank Dr Knut Asmis for the IR spectrum of the H_5O_2^+ ion. One of the authors (MVV) thanks the Alexander von Humboldt foundation for a fellowship and Christian Tuma, Veronika Brázdrová and Dr Alexander Hofmann for help with the numerical computations and Professors J. Hutter, Douglas J. Tobias, Mauro Boero and Dr A. Marco Saitta for useful comments.

References

- (a) G. V. Yukhnevich, E. G. Tarakanova, V. D. Mayorov and N. B. Librovich, *Usp. Khim.*, 1995, **64**, 963; (b) G. V. Yukhnevich, E. G. Tarakanova, V. D. Mayorov and N. B. Librovich, *Russ. Chem. Rev.*, 1995, **64**, 901.
- G. Zundel, *Adv. Chem. Phys.*, 2000, **111**, 1.
- (a) M. V. Basilevsky and M. V. Vener, *Usp. Khim.*, 2003, **72**, 3; (b) M. V. Basilevsky and M. V. Vener, *Russ. Chem. Rev.*, 2003, **72**, 1.
- C. L. Perrin and J. B. Nielson, *Ann. Rev. Phys. Chem.*, 1997, **48**, 511.
- S. Meiboom, *J. Chem. Phys.*, 1961, **34**, 375.
- P. A. Giguère and S. Turrel, *Can. J. Chem.*, 1976, **54**, 3477.
- N. B. Librovich, V. P. Sakun and N. D. Sokolov, *Chem. Phys.*, 1981, **60**, 425.
- M. Tuckerman, K. Laasonen, M. Sprik and M. Parrinello, *J. Chem. Phys.*, 1995, **103**, 150.
- N. Agmon, *Chem. Phys. Lett.*, 1995, **244**, 456.
- R. Vuilleumier and D. Borgis, *J. Chem. Phys.*, 1999, **111**, 4251.
- J. Kim, U. W. Schmitt, J. A. Gruetzmacher, G. A. Voth and N. E. Scherer, *J. Chem. Phys.*, 2002, **116**, 737.
- D. Marx, M. E. Tuckermann, J. Hutter and M. Parrinello, *Nature (London)*, 1999, **397**, 601.
- I. Olovsson, *J. Chem. Phys.*, 1968, **49**, 1063, and references therein.
- A. C. Pavia and P. A. Giguère, *J. Chem. Phys.*, 1970, **52**, 3551.
- D. J. Jones, J. Roziere, J. Penfold and J. Tomkinson, *J. Mol. Struct.*, 1989, **195**, 283.
- K. R. Asmis, N. L. Pivonka, G. Santambrogio, M. Brümmer, C. Kaposta, D. M. Neumark and L. Wöste, *Science*, 2003, **299**, 1375.
- R. Car and M. Parrinello, *Phys. Rev. Lett.*, 1985, **55**, 2471.
- J. Hutter, M. Parrinello, A. Alavi, D. Marx, M. Tuckerman, W. Andreoni, A. Curioni, E. Fois, U. Röthlisberger, P. Giannozzi, T. Deutsch, D. Sebastiani, A. Laio, J. VandeVondele, A. Seitsonen and S. Billeter, *CPMD, 3.5.2*, IBM Research Laboratory and MPI für Festkörperforschung, Stuttgart, 1995–2001.
- R. Rousseau, V. Kleinschmidt, W. Schmitt and D. Marx, *Angew. Chem., Int. Ed. Engl.*, 2004, **43**, 4804.
- G. J. Kearley, F. Fillaux, M. H. Baron, S. Bennington and J. Tomkinson, *Science*, 1994, **264**, 1285.
- S. D. Elliott, R. Ahlrichs, O. Kampe and M. M. Kappes, *Phys. Chem. Chem. Phys.*, 2000, **2**, 3415.
- V. Termath and J. Sauer, *Mol. Phys.*, 1997, **91**, 963.
- R. Ahlrichs, M. Bär, M. Häser, H. Horn and C. Kölmel, *Chem. Phys. Lett.*, 1989, **162**, 165.
- O. Treutler and R. Ahlrichs, *J. Chem. Phys.*, 1995, **102**, 346.
- M. von Arnim and R. Ahlrichs, *J. Comput. Chem.*, 1998, **19**, 1746.
- (a) A. D. Becke, *Phys. Rev. A*, 1988, **38**, 3098; (b) C. Lee, W. Yang and R. G. Parr, *Phys. Rev. B*, 1988, **37**, 785.
- R. A. Kendall, T. H. Dunning Jr. and R. J. Harrison, *J. Chem. Phys.*, 1992, **96**, 6796.
- N. Troullier and J. L. Martins, *Phys. Rev. B*, 1991, **43**, 1993.
- C. Tuma, Diploma Thesis, Humboldt-Universität, Berlin, 2000.
- A. M. Saitta and M. L. Klein, *J. Chem. Phys.*, 2003, **118**, 1.
- R. Resta, *Phys. Rev. Lett.*, 1998, **80**, 1800.
- W. B. Bosma, L. E. Fried and S. Mukamel, *J. Chem. Phys.*, 1993, **98**, 4413.
- M.-P. Gaigeot and M. Sprik, *J. Phys. Chem. B*, 2003, **107**, 10344.
- B. Guillot, *J. Chem. Phys.*, 1991, **95**, 1543.
- S. V. Churakov and B. Wunder, *Phys. Chem. Miner.*, 2004, **31**, 131.
- B. Hudson, A. Warshel and G. R. Gordon, *J. Chem. Phys.*, 1974, **61**, 2929.
- Variations of some CPMD internal parameters (kinetic energy cutoff, convergence criteria for optimisation runs, step length in numerical calculations of harmonic frequencies, etc.) change the energy difference between the $P2_12_1$ and $Pnma$ structures and the value of the imaginary frequency. These variations, however, do not change the relative stability of the structures and the centrosymmetric space group $Pnma$ always has one imaginary frequency.
- M. Boero, Y. Morikawa, K. Terakura and M. Ozeki, *J. Chem. Phys.*, 2000, **112**, 9549.
- J. Borysow, M. Moraldi and L. Frommhold, *Mol. Phys.*, 1985, **56**, 913.
- P. L. Silvestrelli, M. Bernasconi and M. Parrinello, *Chem. Phys. Lett.*, 1997, **277**, 478.
- H. Ahlborn, B. Space and P. B. Moore, *J. Chem. Phys.*, 2000, **112**, 8083.
- D. A. McQuarrie, *Statistical Mechanics*, Harper Collins Publishers Inc., New York, 1973, section 21-1.
- V. M. Zolotarev, B. A. Mikhailov, L. I. Alperovich and S. I. Popov, *Opt. Spectrosc.*, 1969, **27**, 430.
- A. S. Gilbert and N. Sheppard, *Chem. Commun.*, 1971, **7**, 337.
- G. Picotin, J. Roziere, J. Potier and A. Potier, *Adv. Mol. Relax. Processes*, 1975, **7**, 177.
- M. V. Vener, O. Kühn and J. Sauer, *J. Chem. Phys.*, 2001, **114**, 240.
- G. V. Yukhnevich, E. G. Tarakanova, V. D. Mayorov and N. B. Librovich, *J. Mol. Struct.*, 1992, **265**, 237.
- The symmetry of the H_5O_2^+ ion in the $Pnma$ structure depends on the accuracy of the symmetrisation procedure, ϵ . For $\epsilon = 10^{-5}$ au one gets C_i ; for $\epsilon = 5 \times 10^{-2}$ au, C_{2h} . The latter value is of the same order of magnitude of the bond distances correction used in the X-ray study,¹³ $< 5.2 \times 10^{-2}$ au.
- R. Minkwitz, S. Schneider and A. Kornath, *Inorg. Chem.*, 1998, **37**, 4662.
- L. I. Yeh, M. Okumura, J. D. Myers, J. M. Price and Y. T. Lee, *J. Chem. Phys.*, 1989, **91**, 7319.
- J. Sauer and J. Döbler, 2005, to be published.
- J. Dai, Z. Bacic, X. Huang, S. Carter and J. M. Bowman, *J. Chem. Phys.*, 2003, **119**, 6571.
- M. Plazanet, N. Fukushima, M. R. Johnson, A. J. Horsewill and H. P. Trommsdorff, *J. Chem. Phys.*, 2001, **115**, 3241.
- E. Keller, Schakal197, Crystallographic Institute, University of Freiburg, Germany, 1997. See also <http://www.krist.uni-freiburg.de/ki/Mitarbeiter/Keller>.